Cement and Concrete Research 41 (2011) 942–946

Contents lists available at ScienceDirect

Cement and Concrete Research

journal homepage: http://ees.elsevier.com/CEMCON/default.asp

The scratch test for strength and fracture toughness determination of oil well cements cured at high temperature and pressure

Franz-Josef Ulm [a,*], Simon James [b]

[a] Massachusetts Institute of Technology, Cambridge MA 02139, USA
[b] Schlumberger, SRPC, Clamart, France

ARTICLE INFO

Article history:
Received 18 February 2011
Accepted 26 April 2011

Keywords:
Oil well cement (E)
Fracture toughness (C)
Compressive strength (C)
Curing (A)
Temperature (A)

ABSTRACT

Recent advances in scratch test analysis provide new ways to relate measured scratch test properties not only to strength properties but fracture properties of materials as well. Herein, we present an application of such tools to oil well cements cured at high temperatures and pressures. We find a concurrent increase of strength and toughness of different oil well cement baseline formulations which we relate to the water-to-binder ratio for a series of cementitious materials prepared with cement and silica flour. The scratch test thus emerges as a self-consistent technique for both cohesive–frictional strength and fracture properties that is highly reproducible, almost non-destructive, and not more sophisticated than classical compression tests, which makes this 'old' test highly attractive for performance-based field applications.

1. Introduction

The primary objective of well cementing, or the placement of cement in the annulus between the pipe or casing and the rock formation, is zonal isolation. That is, the annular cement sheath must isolate zones containing pressurized fluids from each other and from the surface and maintain this isolation even when the cement sheath is subjected to changes in stress and strain during the operating life of the well. From a mechanics point of view, this objective needs to be met by an appropriate cementitious material that can withstand high temperatures and pressures which are typically encountered in downhole applications. The key to choosing the appropriate material is a method that allows the control of an appropriate material parameter. As in the construction materials industry, the classical parameter in use has been the compressive strength of the material, which is part of the cultural baggage of engineers, be this in infrastructure applications of concrete, or in well-cementing applications. On the other hand, given the objectives of well cementing, one can arguably make the case that the material parameter that controls sealing and stability of the in-situ material does not relate to a limit in strength but rather to a risk of cracking and fracture. A performance-based design of such functions would thus need to consider fracture properties, for instance fracture energy or fracture toughness. The main challenge of fracture toughness properties is that their determination typically requires a much more sophisticated test setup that can deal with fracture size effects inherent to fracture phenomena in brittle and quasi-brittle materials [1], which need to be taken into account in the determination of concrete's fracture properties [2-5]. Presenting such a method that can be used to characterize fracture properties of oil well cements is the focus of this paper. More precisely, using a recently developed fracture approach to analyze the scratch test [6], the aim of this paper is to shed light on the effect of high temperature and pressure on the fracture toughness of a series of baseline oil well cement formulations.

2. Materials and methods

2.1. Materials

The materials considered here are made of class G cement (for composition, see Table 1). As reference, we consider a class G cement hydrated at ambient conditions with no mixed additives. The slurry density of 1.9 g/cc corresponds to a solid volume fraction of 41.5% and a water-to-cement mass ratio of $w/c = 0.44$. With respect to high temperature and pressure applications, two further base-line cement mixes in frequent use in oil well application are investigated. These mixes contain in addition 35% of silica flour (by weight of cement), which is known to react at high temperature and pressure. Silica flour is crystalline silica, containing at least 98% silicon dioxide and with a mean particle size around 20 μm. It is formed by grinding of quartz sand in ball or vibration mills. For comparison with the reference sample the two materials were designed either at the same water-to-cement mass ratio or the same water-to-binder mass ratio. Sample A of slurry density 2.03 g/cc contains 70 vol.% of class G cement and 30 vol.% of silica flour. This corresponds to a solid volume fraction of 50% representative of a water-to-binder mass ratio of $w/b = 0.33$, at a

* Corresponding author.
E-mail address: ulm@mit.edu (F.-J. Ulm).

0008-8846/$ – see front matter © 2011 Elsevier Ltd. All rights reserved.
doi:10.1016/j.cemconres.2011.04.014

Table 1
Typical composition of a class G oil well Portland cement (in mass%).

Composition of Portland cement/class G				
CaO	SiO_2	Al_2O_3	Fe_2O_3	Minor elements
67%	22%	5%	3%	3%

water-to-cement ratio of $w/c=0.45$. Sample series B of slurry density 1.89 g/cc and solid volume fraction of 43.9% has almost the same water-to-binder mass ratio as the reference sample ($w/b=0.43$); yet due to the solid mix of 70.3 vol.% cement and 29.7 vol.% of silica flour ($s/c=0.35$), its water-to-cement ratio is significantly higher, $w/c=0.58$. Finally, each sample series was subjected to different curing conditions: The curing temperature of sample A is 200 °C and the pressure is 20.7 MPa, applied one week and 12 months, respectively. Sample B was cured for one week at 50 °C and then subjected to a temperature of 300 °C and a pressure of 20.7 MPa for one month, two months and three months, respectively. Table 2 summarizes the different mixes and curing conditions and durations considered in this study.

2.2. Scratch hardness and scratch toughness determination

To determine the fracture properties, we use a recently developed analytical framework that allows the determination of the fracture toughness from a series of scratch tests [6]. The scratch test device considered here is a commercially available inclined cutter-blade (back-rake angle $\theta=15°$) of (out-of-plane) width w that is held at a depth d by means of a vertical force F_V. A horizontal force F_T is applied to move the blade. Fig. 1(a) shows a typical result of recorded scratch forces along the scratch path of 5 cm, from which we determine the mean forces and the standard deviation. For each material sample and curing conditions, we carry out such tests with three different widths, $w=2.5,5,10$ mm; and up to six different depths, varying between $d=0.1$ mm and $d=0.35$ mm; typically a total number of 16 scratch tests per sample; thus spanning a large range of w/d ratios between 10 and 100. For the interpretation of the scratch forces we use two complementary approaches:

1. Scratch-Hardness Approach: Following classical approaches to scratch test analysis, that link the applied forces to strength parameters of the scratched materials [7-10], we determine the scratch hardness,

$$F_T \overset{def}{=} H_s \; A_{LB} \tag{1}$$

where F_T is the horizontal force applied to the apparatus; and $A_{LB}=wd$ is the projected load bearing area resisting the horizontal force; that is, the horizontal projection of the contact area between the scratch device and the scratched material. In Fig. 1(b) we plot, for a typical series of scratch tests results, the dependence of the average of F_T of a function of the blade's projected contact area $A_{LB}=wd$. For low values of the projected area, F_T scales linearly with wd, which is indicative of a strength process (see, e.g. [10]); the slope being representative of the scratch hardness of the material; here, for the A-1w sample, $H_s=88.6$ MPa. However, for higher values of wd, deviations from this linear scaling become important, which is attributable to the fracture nature of the scratch test.
2. Fracture Toughness Approach: Following recent developments in the application of linear elastic fracture mechanics (LEFM) to scratch test analysis [6,11], we determine the fracture toughness from the scaling of the driving fracture force F_{eq} with the width-to-depth ratio, w/d,

$$\frac{F_{eq}}{K_c w\sqrt{d}} = \sqrt{2}\left(1+2\frac{d}{w}\right)^{1/2} \tag{2}$$

where K_c is the fracture toughness, and,

$$F_{eq} = \sqrt{F_T^2 + \frac{3}{5}F_V^2} \tag{3}$$

with F_T and F_V the scratch force and the vertical force recorded in the tests. The fracture criterion (2) converges for large values

Table 2
Tested Oil-well cement samples. Mix formulation and temperature–pressure curing conditions.

		Reference	Sample A	Sample B
Slurry density	g/cc	1.9	2.03	1.89
w/c	M%	44	45	58
w/b	M%	44	33	43
s/c	M%	0	35	35
			Curing Conditions	
Temperature	°C	25	200	1 week 50, then 300
Pressure	MPa	Atm.	20.7	20.7
Duration	week		1 (A-1w)	4 (B-4w)
	week		51 (A-51w)	8 (B-8w)
	week			12 (B-12w)

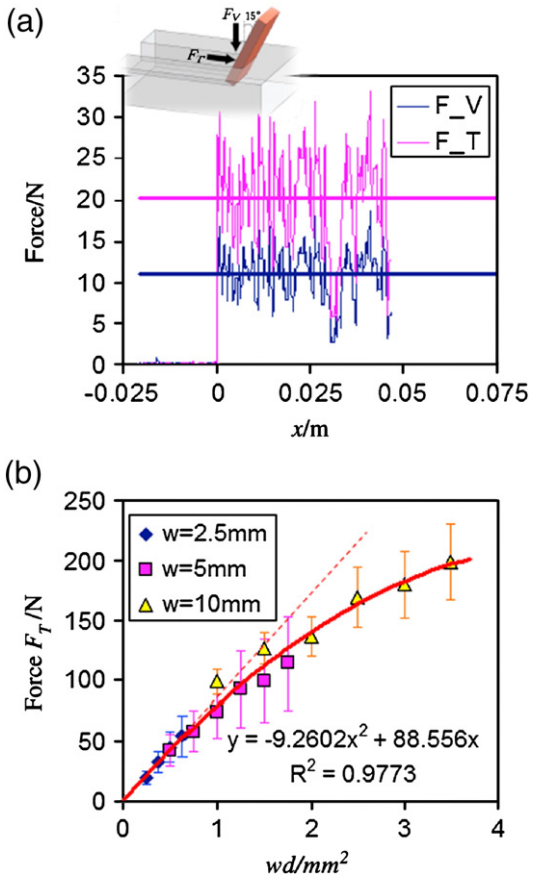

Fig. 1. Force measurements in a scratch test on Sample A–1w: (*a*) Scratch force F_T and vertical force F_V over a 5 mm scratch length in scratch test $w=2.5$ mm, $d=0.1$ mm. Straight lines represent mean values. (*b*) Mean scratch forces, F_T, vs. projected contact area, wd, in 16 scratch tests carried out with three different widths, $w=2.5,5,10$ mm, operated to different depths, $d=0.1-0.35$ mm. Error bars represent standard deviations.

of w/d to a form that allows the determination of the fracture toughness from:

$$w/d >> 1 : \frac{F_{eq}}{\sqrt{2}} = K_c w\sqrt{d} \tag{4}$$

In Fig. 2 we apply this fracture criterion to the test results of one sample. In particular, in Fig. 2(a) we plot $F_{eq}/\sqrt{2}$ vs. $w\sqrt{d}$. Two observations deserve particular attention: First, the straight-line fits confirm the linearity between F_{eq} and $w\sqrt{d}$ as predicted by the LEFM model (4). Moreover, the slope, which is representative for large values of w/d of the fracture toughness, decreases with the increase of the scratch width, w. To explore this scaling, we plot in Fig. 3(b) the same data set, in terms of $F_{eq}\Big/\left(w\sqrt{2d}\right)$ vs. w/d. As predicted by LEFM, $F_{eq}\Big/\left(w\sqrt{2d}\right)$ converges with w/d to a constant value that is representative of the fracture toughness. The mean value for the considered sample is $K_c = 0.83 \pm 0.10\ \mathrm{MPa}\sqrt{\mathrm{m}}$ obtained by averaging $F_{eq}\Big/\left(w\sqrt{2d}\right)$ for $w/d > 10$. The technique has been validated for several materials, including cement paste, sandstone, limestone, and so on [6,11].

3. Results

Table 3 lists for the materials and curing conditions considered the scratch hardness, H_s, and fracture toughness, K_c, determined from each series of scratch tests as described here before; together with the unconfined compressive strength, UCS, determined on cylinder samples. The data display a fair amount of consistency: the general trend is that both the scratch hardness (Fig. 3(a)) and the fracture toughness (Fig. 3(b)) increase with the compressive strength, UCS. Two observations deserve particular attention: The first relates to the positive correlation of H_s with UCS, the second to the correlation of H_s or UCS with the fracture toughness.

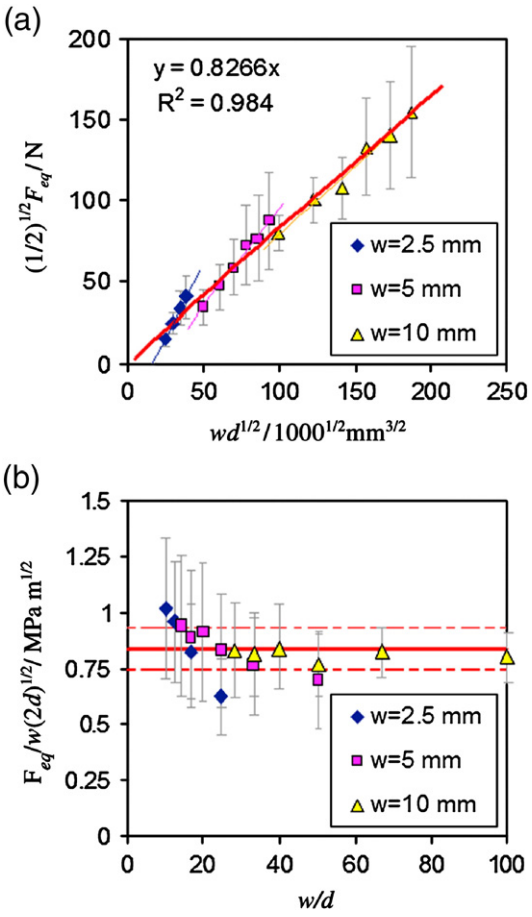

Fig. 2. Fracture Toughness determination from 16 scratch tests on sample A-1w carried out with 3 different widths, $w = 2.5, 5, 10$ mm, and different depths, $d = 0.1 - 0.35$ mm: (a) Fracture force $F_{eq}/\sqrt{2}$ vs. $w\sqrt{d}$. The slope in this figure is representative of fracture toughness for large values of w/d (Eq. 4). (b) Fracture toughness plot, $F_{eq}\Big/\left(w\sqrt{2d}\right)$ vs. w/d, showing a convergence for large values of w/d. Error bars in the figure are representative of standard deviations.

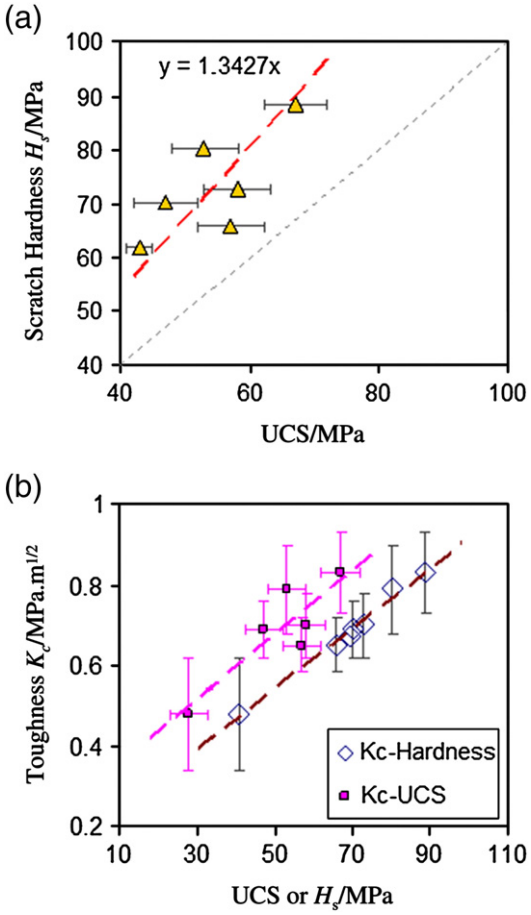

Fig. 3. Results: (a) Scratch hardness, H_s, vs. unconfined compressive strength, UCS. (b) Fracture toughness, K_c, vs. UCS or H_s.

3.1. Cohesive–frictional strength behavior

The positive correlation of H_s with UCS (Fig. 3(a)) has been recently identified to relate to the cohesive–frictional nature of the scratched material [10]. More precisely, from a straightforward dimensional analysis for cohesive–frictional materials,

$$\frac{H_s}{UCS} = \Pi_S(\mu) \tag{5}$$

Table 3
Results: UCS = unconfined compressive strength (Mean ± St.Dev. of 5 tests); H_s = Scratch hardness; K_c = fracture toughness. (*) Cohesion C is determined from Eq. (6) under the assumption of a constant friction angle. Details provided in the text.

Sample	T/°C	p/MPa	UCS/MPa	H_s/MPa	C/MPa(*)	K_c/MPa.m$^{1/2}$
Reference	25	p_{atm}	43 ± 2	61.8	17.3	0.66 ± 0.05
A-1w	200	20.7	67 ± 5	88.6	24.8	0.83 ± 0.10
A-51w	200	20.7	53 ± 5	80.3	22.5	0.79 ± 0.11
B-4w	300	20.7	57 ± 5	65.8	18.4	0.65 ± 0.07
B-8w	300	20.7	47 ± 5	70.2	19.7	0.69 ± 0.07
B-12w	300	20.7	58 ± 5	72.9	20.4	0.70 ± 0.08

with $\mu = \tan\varphi$ the friction coefficient, and φ the friction angle (in the sense of a Mohr–Coulomb material; [13]). Such relations have been derived recently and show that for values of $H_s/UCS > 1 + \sin\theta = 1.26$ (with $\theta = 15°$ the back-rake angle), there is internal friction at play. In fact, the mean H_s/UCS ratio for all samples is 1.36. We use the following two analytical relations relevant for a Mohr–Coulomb material (for details, see Ref. [10]),

$$H_s = 2C\frac{\cos\varphi\left(1-\sin^2\theta\right)}{1-\sin\theta\cos\varphi\sqrt{1+(\tan\varphi\sin\theta)^2}-\sin\varphi\cos^2\theta} \quad (6)$$

$$UCS = 2C\frac{\cos\varphi}{1-\sin\varphi} \quad (7)$$

with C the cohesion; to determine from $H_s/UCS = 1.36$ a friction coefficient of $\mu = 0.266$; that is a friction angle of $\varphi = 15.2°$. This value is in very good agreement with previously reported friction angles for oil cement slurries obtained by triaxial testing (confined compressive strength tests) [14,15]. While there is obviously some variability in H_s/UCS ratios between samples, the results provide some insight that the dominant source of different scratch hardness is the cohesion of the material. For illustration, Table 3 also lists the cohesion values, C, determined with a constant friction angle of $\varphi = 15.2°$ from Eq. (6). What thus emerges is that for the same water-to-binder (w/b) mass ratio (compare Reference sample to Sample B), cementitious materials achieve similar values of cohesion that are only slightly affected by the high temperature–pressure curing conditions. This observation is also consistent with the fact that the lower w/b — ratio of the A sample compared to both the reference sample and B-samples entails a higher cohesion. Compared to this dominating effect related to the mix design, the duration of temperature–pressure curing conditions appear, as a second order effect, to affect the frictional behavior. For instance, the H_s/UCS ratio for the A-samples increases from 1.32 to 1.52 due to prolonged curing (compare sample A-1w and A-51w), which corresponds to an increase of the friction coefficient (friction angle) from $\mu_{A-1w} = 0.172$ ($\varphi = 9.8°$) to $\mu_{A-51w} = 0.517$ ($\varphi = 29.6°$). A similar trend is found for samples B-4w and B-8w (but less so for B-12w). Such a variability of the friction angle has also been found in triaxial testing of oil cement slurries [16,17], for which the method proposed is an attractive alternative.

3.2. Toughness–ductility behavior

A first observation is that the scratch toughness of the reference sample, $K_c = 0.66 \pm 0.05$ MPa$\sqrt{\text{m}}$, almost coincides with fracture toughness values obtained by notched three-point bending tests for large $w/c = 0.5$ cement paste specimen, $K_c = 0.67$ $MPa\sqrt{\text{m}}$ [2], or by means of extrapolation techniques that avoid interference with specimen size, $K_c = 0.65$ $MPa\sqrt{\text{m}}$ [3]. While this observation provides some credibility to the method, the more important observation is the positive correlation between fracture toughness, K_c, on one hand, and UCS or scratch hardness, H_s, on the other hand (Fig. 3(b)). In particular, as for scratch hardness, we observe that materials with same w/b ratio display almost the same fracture toughness (compare Reference with Samples B) independent of the different curing conditions. In return, materials with lower w/b ratio exhibit a significant higher fracture toughness (compare Sample A with Reference Sample or Sample B). For many materials, such an increase in fracture toughness is often associated with a higher brittleness or lower ductility. However, the concurrent increase in fracture toughness and hardness, $K_c \sim H_s$, for the samples considered here is an indication that the ductility of the material is preserved across all samples. A good means to quantify the ductility is the characteristic size of the fracture process zone (FPZ), which we estimate from,

$$r_p = \frac{1}{2\pi}\left(\frac{K_c}{C}\right)^2. \quad (8)$$

The values for r_p calculated for each sample and curing condition from Table 3, vary indeed little around the mean of $r_p = 0.20 \pm 0.02$ mm, without any pronounced relation with strength or hardness. This means that the ductility of the materials tested here is, in first order, independent of the specific mix formulation. Finally, it is useful to note that the size of this fracture process zone is much smaller than the characteristic size of the scratching defined by the blade width w, which a posteriori justifies the use of LEFM for scratch test analysis, i.e. Eqs. (2)–(4).

4. Concluding remarks

While the scratch test is probably one of the oldest techniques in the characterization of mechanical material properties, recent advances in scratch test analysis provide a means to relate measured scratch test properties to both strength and fracture properties of the material. In contrast to classical fracture tests, such as notched beam tests or double-cantilever tests [3-5,12], where the size of the fracture process zone is often of an order that impedes the direct determination of size-independent fracture properties, the scratch test is an attractive alternative. In the scratch test, the fracture process zone expands into the bulk material, but it does not interfere with size and boundary of the specimen as this is well known for e.g. notched beam tests [3]. Carrying out a series of scratch tests with different blade widths and depths thus provides a means to determine both the scratch hardness and the fracture toughness with high accuracy. Such a technique is invaluable to identify functional relations for material design, as shown here for oil well cements:

1. The key material design parameter for cohesion and fracture toughness is the water-to-binder ratio (w/b), not the water-to-cement ratio (w/c). While this conclusion is far from original for strength properties, as it relates to the amount of hydration products that form in the hardened material, we show that this functional relation also holds for fracture properties of cementitious materials prepared with cement and silica flour, when cured at high temperature and pressure so that the quartz reacts. The concurrent increase in fracture toughness and cohesion as related to the water-to-binder ratio (w/b) is such that the ductility is preserved.
2. Prolonged high temperature and high pressure curing induces some second order effects, manifesting themselves by a frictional enhancement together with a softening of cohesion and the fracture toughness. Such phenomena are often attributable to coarsening of the microstructure [18,19], that warrant further investigation; but which go beyond the scope of this investigation.

The scratch test thus emerges as a self-consistent technique for both cohesive–frictional strength and fracture properties that are highly relevant for oil-well cementing applications. The fact that it is highly reproducible, almost non-destructive, and not more sophisticated than classical compression tests, makes this “old” test highly attractive for performance-based field applications. This conclusion not only holds for high-temperature/high pressure oil-well cement applications, but also for normally cured cementitious materials, as the good agreement between the reference sample and literature value shows. One could therefore suggest the scratch test for standardized quality control purposes of fracture properties of cementitious materials.

Acknowledgment

Research carried out within the framework of an MIT—Schlumberger sponsored project. The experimental scratch data were developed by Epslog Engineering SA, Belgium. We are grateful to the team at MIT (Drs. J.A. Ortega, R. Pellenq, H.M. Jennings, A. Dirieh, A-T. Akono) and Schlumberger (Drs. J. Thomas, F. Auzerais) for fruitful discussions.

References

[1] Z.P. Bažant, P. Jaime, Fracture and Size Effect in Concrete and Other Quasibrittle Materials, CRC Press, Boca Raton and London, 1998.
[2] B. Cotterell, Y.-W. Mai, Crack growth resistance curve and size effect in the fracture of cement paste, Journal of Materials Science 22 (1987) 2734–2738.
[3] X.Z. Hu, F. Wittmann, Size effect on toughness induced by crack close to free surface, Engineering Fracture Mechanics 65 (2–3) (2000) 209–211.
[4] K. Duan, X.Z. Hu, F.H. Wittmann, Boundary effect on concrete fracture and non-constant fracture energy distribution, Engineering Fracture Mechanics 70 (2003) 2257–2268.
[5] X.Z. Hu, An asymptotic approach to size effect on fracture toughness and fracture energy of composites, Engineering Fracture Mechanics 69 (5) (2002) 555–564.
[6] A.-T. Akono, F.-J. Ulm, Scratch test model for the determination of fracture toughness, Engineering Fracture Mechanics 78 (2011) 334–342.
[7] J.A. Williams, Analytical models of scratch hardness, Tribology International 29 (1996) 675–694.
[8] T. Richard, E. Detournay, A. Drescher, P. Nicodeme, D. Fourmaintraux, The scratch test as a means to measure strength of sedimentary rocks, SPE/ISRM 47196 (1998).
[9] G. Schei, E. Fjær, E. Detournay, C.J. Kenter, G.F. Fuh, The scratch test: an attractive technique for determining strength and elastic properties of sedimentary rocks, SPE 63255 (2000).
[10] R. Bard, F.-J. Ulm, Scratch hardness strength solutions for cohesive–frictional materials, International Journal for Numerical and Analytical Methods in Geomechanics (2010), doi:10.1002/nag.1008.
[11] A.-T. Akono, P.M. Reis, F.-J. Ulm, Scratching as a fracture process: From butter to steel, Physics Review Letters 69 (2002) 1845–1852.
[12] L.E.T. Ferreira, T.N. Bittencourt, J.L.A.O. Sousa, R. Gettu, R-curve behavior in notched beam tests of rocks, Engineering Fracture Mechanics 69 (2002) 1845–1852.
[13] F.P. Ganneau, G. Constantinides, F.-J. Ulm, Dual-indentation technique for the assessment of strength properties of cohesive–frictional materials, International Journal of Solids and Structures 43 (2006) 1727–1745.
[14] M. Thiercelin, C. Baumgarte, D. Guillot, A soil mechanics approach to predict cement sheath behaviour, SPE 47375 (1998).
[15] C. Capacho, F. Baquero, K. Ravi, J. Vela, Cement design to optimize production in a highly active waterdrive reservoir, SPE 107701 (2007).
[16] M. Bosma, K. Ravi, W. van Driel, G.J. Schreppers, Design approach to sealant selection for the life of the well, SPE 56536 (1999).
[17] H.B. Ramirez, A. Santra, C. Martinez, A.X. Ramos, Gas-migration control and mechanical properties improvement with a right angle-set slurry design to be applied in a production cementing-job for Ecuador, SPE 123085 (2009).
[18] M.J. DeJong, F.-J. Ulm, The nanogranular behavior of C–S–H at elevated temperature (up to 700 °C), Cement and Conrete Research 37 (1) (2007) 1–12.
[19] C.P. Bobko, B. Gathier, J.A. Ortega, F.-J. Ulm, L. Borges, Y.N. Abousleiman, The nanogranular origin of friction and cohesion in shale—A strength homogenization approach to interpretation of nanoindentation results, International Journal for Numerical and Analytical Methods in Geomechanics (2010), doi:10.1002/nag.984.